Journal of Catalysis **205,** 168–176 (2002)
doi:10.1006/jcat.2001.3423, available online at http://www.idealibrary.com on IDEAL®

Electrospray Ionization–Mass Spectrometry in the Enantioselective Hydrogenation of Ethyl Pyruvate Catalyzed by Dihydrocinchonidine Modified Pt/Al_2O_3 in Acetic Acid

Mihály Bartók,*,†,[1] Katalin Balázsik,* György Szöllösi,* and Tibor Bartók‡

*Organic Catalysis Research Group of the Hungarian Academy of Sciences, Dóm tér 8, H-6720 Szeged, Hungary; †Department of Organic Chemistry, University of Szeged, Dóm tér 8, H-6720 Szeged, Hungary; and ‡Analytical Laboratory of the Cereal Research Institute, P.O.Box 391, H-6701 Szeged, Hungary

Received June 29, 2001; revised August 31, 2001; accepted August 31, 2001

The enantioselective hydrogenation of ethyl pyruvate (EtPy) on Pt–alumina (E 4759), Pt black, and Pt black + alumina (mixture) catalysts modified by dihydrocinchonidine (DHCD) in acetic acid was studied by electrospray ionization–mass spectrometry (ESI–MS). Application of the ESI–MS technique led to the recognition of a novel-type compound, $O^+[Al(OAc)_2]_3$ (oxonium ions). The effect of the DHCD concentration, temperature, and oxonium cations on the reaction rate and the enantioselectivity has been studied. Using the Engelhard 4759 catalyst in acetic acid under mild experimental conditions (room temperature, hydrogen pressure 1 bar, DHCD concentration 0.01 mM/L) an optical yield of 92% can be achieved. The high enantioselectivity is accompanied by the following turnovers: EtPy/DHCD > 43,000, $EtPy/Pt_{surface} > 1000$, $TOF = 1–2\ s^{-1}$, and $DHCD/Pt_{surface}$ ratio = 0.0072. The enantioselectivity reducing factor is identified by ESI–MS as the gradual hydrogenation of the quinoline skeleton of DHCD that becomes more pronounced with increasing temperature and hydrogenation time. The discovery of oxonium cations, the extremely low $DHCD/Pt_{surface}$ ratio, and the new data obtained by the Pt black + alumina mixture made possible an interpretation of the mechanism of the heterogeneous enantioselective hydrogenation of α-ketoesters. © 2002 Elsevier Science

Key Words: **hydrogenation; enantioselective; Pt/Al_2O_3; dihydrocinchonidine; ethyl pyruvate; ESI–MS; intermediate; oxonium cations.**

INTRODUCTION

Enantiomers play an extremely important role in the synthesis of pharmaceuticals, agrochemicals, flavors, and fragrances. Studies on heterogeneous asymmetric catalytic reactions involving enantiomers have therefore recently gathered considerable momentum (1–4). The enantioselective hydrogenation of α-ketoesters is one of the best known examples of such reactions (5, 6). Of these, the enantioselective hydrogenation of ethyl pyruvate (EtPy) resulting in the formation of (*R*)-ethyl lactate (EtLt) with an enantioselectivity of 97% (7, 8) on an alumina-supported platinum catalyst modified with dihydrocinchonidine (DHCD) has been studied in detail (Scheme 1).

The determination of the optimal parameters of (*R*)-EtLt production and the interpretation of the reaction mechanism is still an on-going process (see Refs. 9–15).

The following literature data are considered on the interpretation of the chiral hydrogenation of pyruvates. (i) the particle size and morphology of the $Pt–Al_2O_3$ catalyst (5, 6, 8, 13, 16–22), (ii) how DHCD is adsorbed and on which surface sites (8, 16, 23–26), (iii) the adsorption of DHCD and pyruvate (9, 23, 24, 26–30), (iv) the conformation of DHCD (15, 31–33), (v) the stability of DHCD as a chiral modifier under the conditions of the hydrogenation (15, 34), (vi) the formation of the intermediate complex in solution and/or on the surface of the catalyst (5, 6, 27, 35–37), (vii) the structure of the intermediate responsible for chirality (5, 9, 23, 27, 35, 36, 38–42), (viii) the roles of DHCD concentration and of the DHCD/Pt and pyruvate/Pt ratios (6, 12, 43), and (ix) the results of kinetic reaction studies (35, 25, 43–45).

The most important conclusions of these investigations on the enantioselective hydrogenation of EtPy can be summarized as follows: (i) the highest enantioselectivities can be reached on the Pt–alumina catalyst having its main particle size in the range of 1.5–4 nm; (ii) the best solvent was found to be AcOH; (iii) the best modifiers are the cinchona alkaloids which have to be present in an optimal concentration; (iv) the structure of the surface complex responsible for the chiral induction is the cinchona alkaloid "anti-open" conformer–pyruvate 1 : 1 complex; (v) the reaction rate of the enantioselective reaction is significantly higher than the rate of the racemic hydrogenation; the enantioselectivity and the reaction rate have a maxima as a function of the modifier concentration; (vi) under optimal reaction conditions the decrease in ee can be ascribed to the hydrogenation of the modifier.

[1] To whom correspondence should be addressed. Fax: 36-62-544-200. E-mail: bartok@chem.u-szeged.hu.

0021-9517/02 $35.00

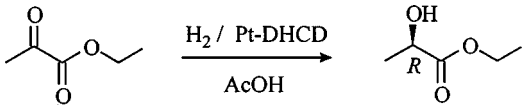

SCHEME 1

The major aim of this work is the presentation of our new experimental results on the asymmetric hydrogenation of EtPy on the Pt–alumina catalyst in acetic acid, in the presence of DHCD, made possible mainly by the application of electospray ionization–mass spectrometry (ESI–MS and ESI–MS/MS) (46–48). In this investigations ESI–MS is used for the identification of the intermediates, different adducts, and side products formed in the reaction. A great advantage of ESI–MS as compared with other ionization methods is that, due to the mildness of the ionization process, sample fragmentation is less severe. In most cases intact molecular ions are also detected in the sample.

EXPERIMENTAL

Materials

Cinchonidine (CD), AcOH, MeOH, and EtOH were purchased from Fluka. EtPy (Fluka) was distilled before use to attain 99.5% purity. DHCD was prepared by hydrogenation of CD (Pd/C, 1 N H_2SO_4/H_2O, 1 bar, 298 K) and used after crystallization.

Based on the data in the literature, among several catalysts the one most often used is Engelhard 4759 (E 4759). The properties of this contact catalyst are the following (5): Pt content, 5% (w/w); Pt dispersion, as received, 38%; after pretreatment, 27% (49); mean Pt particle size, 4.5 nm; support, γ-Al_2O_3; specific surface area, 168 $m^2\ g^{-1}$; mean pore radius, 2 nm; specific pore volume, 0.27 mL g^{-1}. E 4759 was pretreated before use in a fixed-bed reactor by flushing with 30 mL min^{-1} helium at 300–673 K for 30 min and 30 mL min^{-1} hydrogen at 673 K for 100 min. After cooling to room temperature in hydrogen, the catalyst was flushed with helium for 30 min and stored in air before use.

Platinum black (Aldrich 20,591-5), aluminum oxide (Aldrich 19,997-4), and aluminum acetates (Aldrich 28,982-5 and 29,485-3) were used as received.

Hydrogenation

Hydrogenation was performed in an atmospheric bath reactor or in a Berghof Bar 45 autoclave at room temperature (298 K). The catalytic system including the catalyst and 2 mL of AcOH was purged three times with hydrogen after prehydrogenation (30 min). The calculated amount of modifier and 0.1–2 mL of EtPy were introduced and stirred (1200 rpm) in the presence of hydrogen for the required reaction time (usually 10–50 min). The standard conditions were: 25 mg E 4759, 2 mL AcOH, 0.01 mM/L DHCD, 1 bar H_2, 296 K, 1200 rpm, and 0.1 mL EtPy. The quantification of conversion and ee were based on GC data. The product identification and the enantiomeric excess $[ee\% = ([R]-[S])\times 100/([R]+[S])]$ were monitored by gas chromatography (HP 5890 GC-FID, 30-m-long Cyclodex-B capillary column, uncertainty $\pm 2\%$).

ESI–MS Measurements

A Hewlett–Packard HP 5989 B MS Engine quadrupole mass spectrometer equipped with a high-energy dinode detector and an atmospheric pressure ionization–electrospray (API–ES) interface (HP 59987 A) were used. To perform ES experiments, samples were dissolved separately in a mixture of MeOH/AcOH or EtOH/AcOH (98/2 v/v) and introduced into the ES ion source by using a Harward Type 22 syringe pump at a flow rate of 20 μl min^{-1}. A fine spray was formed by applying nitrogen as nebulizer gas at a pressure of 135 kPa. Nitrogen drying gas (heated to 563 K) was used at a flow rate of 8 L min^{-1} to facilitate solvent evaporation from the droplets. After tuning, mass spectra of reaction mixtures were acquired by applying a capillary exit voltage (CapEx) of 100 V. The instrument was run in SCAN mode at above 0.1 mM/L DHCD concentration. When the concentration of DHCD was in the range of 0.001–0.1 mM/L selected ion monitoring (SIM) was applied. Case samples were prepared for ESI–MS in the following way: after removing by rotary vacuum evaporation the acetic acid content of the hydrogenation samples obtained after incomplete and complete conversion, the samples were dissolved separately in a mixture of 2×0.5 mL of MeOH/H_2O/AcOH (80/18/2 v/v). Product composition is unaffected by the conditions of ESI below a CapEx of 100 V; above 100 V, fragmentation processes may be set off. Relative peak intensities in the individual samples to be analyzed were determined under completely identical ESI conditions, rendering comparison of the compositions of samples hydrogenated under different conditions. It must be noted that peak intensities determined by ESI–MS were compared only for DHCD and its hydrogenated derivatives.

ESI–MS/MS Measurements

ESI–MS/MS measurements were run on a FINNIGAN TSQ7000 tandem mass spectrometer equipped with a home-built nanospray source (50), where a pulled, gold-coated capillary was used. The high voltage at the capillary was set at 1100 V. The instrument was run in product ion mode. The mass range of Q3 was set at 10–1500 u with a SCAN time of 1.5 sec. Argon was used as collision gas at a pressure of 0.33 Pa. The collision energy was manually set in the range 20–35 eV.

RESULTS AND DISCUSSION

Since the effects of the reaction conditions of hydrogenation on enantioselectivity have never been studied

by ESI–MS, we had to repeat several experiments which had already been accomplished in the course of the optimization of (*R*)-EtLt production.

Unknown Adducts in the Reaction Mixture

The experimental program included the determination of the reaction rate and enantioselectivity as the functions of DHCD concentration, temperature, and EtPy concentration. The ESI–MS spectrum of the raw product of the hydrogenation reaction was recorded, and the peaks with unknown m/z values were identified by ESI–MS/MS (14).

The two representative spectra shown in Figs. 1a and 1b (recorded at different DHCD concentrations) were selected from a great number of ESI–MS spectra; peaks so far identified are listed in Table 1. The presence of MeOH and EtOH in some adducts is due to their use as solvents in ESI. Adducts containing solvent molecules are not generated under the conditions of ESI: they are formed in the course of the dilution of the reaction product (with MeOH or EtOH), during the preparation of the samples for the MS measurements.

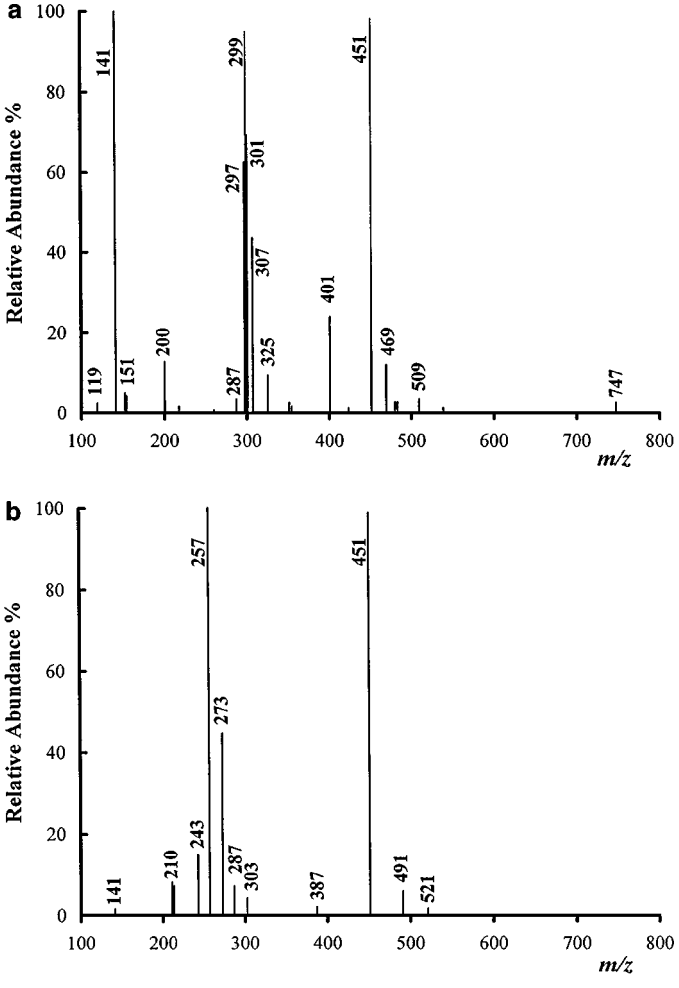

FIG. 1. Positive ion ESI–MS (CapEx 100V) of the EtPy hydrogenation product (25 mg E 4759, 2 mL AcOH, 1 bar H_2, 298 K, 0.1 mL EtPy). (a) 3 mM/L DHCD and (b) 0.014 mM/L DHCD. For abbreviations, see Table 1.

TABLE 1

Adducts Detected by Positive ESI–MS and ESI–MS/MS [m = 23 (Na), 39 (K), 32 (MeOH), 46 (EtOH), 116 (EtPy), 118 (EtLt), 296 DHCD), 71 (Py), 73 (Lt), 43 (Ac)][a]

m/z	Adducts
119	$[EtLt + H]^+$
141	$[EtLt + Na]^+$
151	$[HHCD + 2H]^{2+}$
154	$[DDHCD + 2H]^{2+}$
200	$[THCD + 2MeOH + 2H_2O + 2H]^{2+}$
201	$[HHCD + 2MeOH + 2H_2O + H]^+$
257	$[EtPy + EtLt + Na]^+$
273	$[EtPy + EtLt + K]^+$
287	$[2EtPy + MeOH + Na]^+$
297	$[DHCD + H]^+$
299	$[THCD + H]^+$
301	$[HHCD + H]^+$
303	$[2EtPy + MeOH + K]^+$
307	$[DDHCD + H]^+$
371	$[3EtPy + Na]^+$
373	$[2EtPy + EtLt + Na]^+$
387	$[3EtPy + K]^+$
401	$[HHCD + 2MeOH + 2H_2O + H]^+$
403	$[3EtPy + MeOH + Na]^+$
451	$[O\{Al(OAc)_2\}_3]^+$
469	$[451 + H_2O]^+$
483	$[451 + MeOH]^+$
491	$[2EtPy + 2EtLt + Na]^+$
509	$[O\{Al(OAc)_2 \cdot Al(OPy \cdot OLt)\}]^+$
515	$[451 + 2MeOH]^+$
521	$[3EtPy + EtLt + MeOH + Na]^+$
543	$[451 + 2EtOH]^+$
547	$[451 + 3MeOH]^+$
551	$[4EtPy + 2MeOH + Na]^+$
567	$[O \cdot Al(OAc)_2 \cdot Al(OPy)_2 \cdot Al(OLt)_2]^+$
589	$[451 + 3EtOH]^+$
719	$[6EtPy + Na]^+$
747	$[451 + DHCD]^+$
751	$[6EtPy + MeOH + Na]^+$

[a] Abbreviations used: EtPy, ethyl pyruvate; EtLt, ethyl lactate; DHCD, dihydrocinchonidine; THCD, tetrahydrocinchonidine; HHCD, hexahydrocinchonidine; DDHCD, dodecahydrocinchonidine; Ac, acetyl; Py, pyruvyl; Lt, lactyl.

Inspection of the ESI–MS spectra, surprisingly, revealed a large number of peaks and a high dependence of their positions (m/z) on DHCD concentration. The adducts presented in Table 1 can be classified into four groups according to their type: (i) DHCD and its hydrogenated derivatives, (ii) the adducts of EtPy and its oligomers, (iii) EtLt and its adducts, and (iv) oxonium compounds formed from alumina.

Identification of the peak with $m/z = 451$ was quite problematic and finally led to the recognition of a novel-type

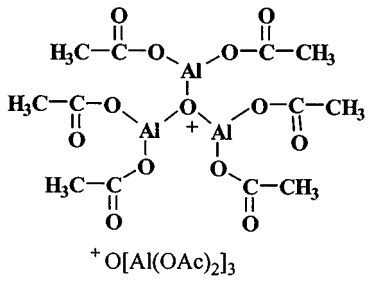

FIG. 2. The structure of $m/z = 451$.

compound (51) (Fig. 2). As shown in Table 1, the oxonium cation with $m/z = 451$ was identifiable on the basis of several adducts, the most important of these being the DHCD adduct of the oxonium cation, $m/z = 747$. This compound probably plays a role in the development of the chiral environment on the catalyst surface. Na^+ and K^+ adducts were not generated by the intentional addition of Na^+ and K^+ ions but are contaminants present in all components of the system (catalyst, solvents, glass reactor, etc.). Studies on the effects of the various adducts on enantioselectivity may constitute the subject of further experiments.

The Effect of DHCD Concentration

The basic experimental data, revealing for the first time that the DHCD concentration has a significant influence on the rate and selectivity of the enantioselective hydrogenation of EtPy, were published by Blaser and co-workers in the early 1990s (43, 52). However, there are no data published on the effect of the DHCD concentration on the reaction rate and enantioselectivity in AcOH at 1 bar H_2 pressure on the E 4759 catalyst. This study had to be carried out, as such experimental data may be essential in studying the reaction mechanism. Our pertinent experimental results are summarized in Figs. 3 and 4a and 4b and Table 2.

The achievement of high optical yields is dependent on an optimal DHCD concentration adjusted to the experimental conditions. The function describing the dependence on DHCD concentration of the reaction rate has maxima. For the interpretation of these maxima there are two explanations in the literature (12, 43). Blaser *et al.*, on the basis of their kinetic study, explained this phenomenon by the so-called "three-site model" (43), while LeBlond *et al.* (12) interpreted it by the change of the optimal adsorption geometry of DHCD at higher concentrations of the modifier.

The experimental data (Fig. 4a) indicate that, under the standard conditions described in the Experimental section, the minimal amount of DHCD necessary for the achievement of maximal enantioselectivity is in the range of 0.001–0.01 mM/L. For this reason additional investigations were necessary in this DHCD concentration range. The

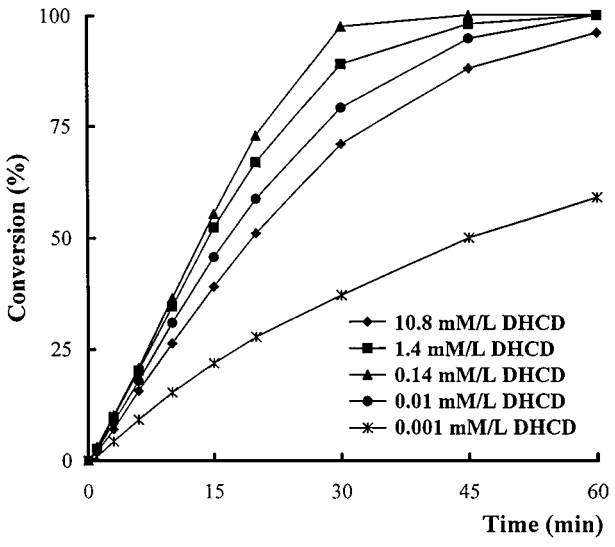

FIG. 3. Hydrogenation of EtPy on DHCD-modified platinum (25 mg E 4759, 1 bar H_2, 2 mL AcOH, 0.5 mL EtPy, 296 K, 1200 rpm). For abbreviations, see Table 1.

relationship between hydrogenation time, conversion, DHCD concentration, and enantioselectivity is shown in Fig. 4b and in Table 2.

Although there have been indications related to the cause of reduced enantioselectivity when the reaction time and conversion were increased (5, 6, 12), the progress of the formation of hydrogenated DHCD derivatives is experimentally confirmed by the ESI–MS data shown in Table 3.

According to the data presented in Table 3, in the course of the hydrogenation of EtPy the quinoline skeleton of DHCD hydrogenates also. The ratio of hydrogenated cinchonas increases with the increasing conversion of EtPy. Since the adsorption strength of hydrogenated cinchonas is considerably lower than that of DHCD, they are easily desorbed at high DHCD concentrations, whereas at low DHCD concentrations (below 0.1 mM/L) enantioselectivity will decrease because there is not sufficient DHCD present to produce optimal surface coverage. The same is confirmed by the results obtained when the

TABLE 2

Time of Reaction, Conversion, and Enantioselectivity as Functions of DHCD Concentration for Hydrogenation of EtPy[a]

DHCD (mM/L)	Time (min)	Conversion (%)	ee (%)
0.001	90	64	39
0.002	90	70	51
0.006	40	90	85
0.01	25	96	88
0.01	15	82	91

[a] For conditions, see Fig. 4.

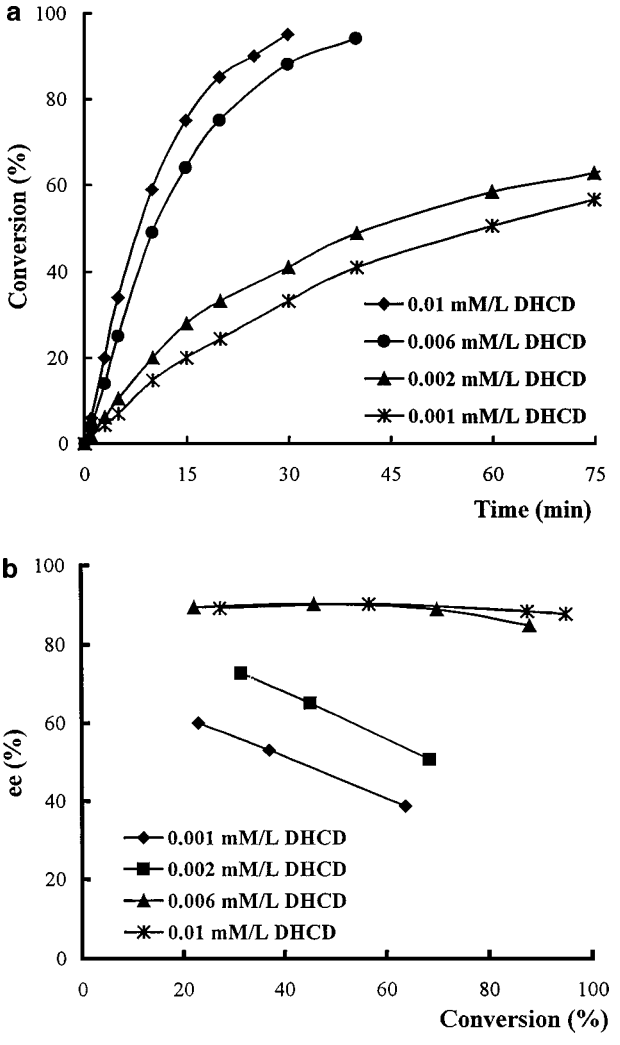

FIG. 4. (a, b) Hydrogenation of EtPy on DHCD-modified platinum (25 mg E 4759, 1 bar H_2, 2 mL AcOH, 0.1 mL EtPy, 296 K, 1200 rpm). For abbreviations, see Table 1.

amount of EtPy was increased under identical experimental conditions, as shown in Fig. 5.

The data in Table 3 also confirm that enantioselectivity of 92–93% can be achieved under very mild experimental conditions (hydrogen pressure: 1 bar, room temperature, short reaction time) if an optimal chiral environment is created.

As previously mentioned, these investigations permitted the determination of the minimal amount of DHCD required for obtaining the maximal enantioselectivity.

The Effect of Temperature

The role of temperature was first studied under relatively severe experimental conditions (high hydrogen pressure and DHCD concentration) (35, 53), and important conclusions were drawn. As far as we know, the results obtained under the mild experimental conditions applied by us (hydrogen pressure 1 bar, DHCD concentration 0.001–0.1 mM/L, temperature 263 K, 273 K) have not been published previously. Our experimental results are summarized in Figs. 6 and 7. Reaction times employed in the experiments are presented in Fig. 6, and the corresponding conversions are listed in Table 4.

Naturally, it was to be expected that the hydrogenation rate of EtPy would decrease as a consequence of reducing temperature. The most important observation is, however, that the hydrogenation rate of the quinoline ring of DHCD decreased to an even higher extent: the hydrogenation of DHCD was not detectable at all (DHCD 0.001 mM/L, EtPy conversion 32%, reaction time 150 min) while the formation of (*R*)-EtLt still proceeded with high (80%) enantioselectivity under these conditions.

TABLE 3

Relative Abundances of $[M + H]^+$ Ions in the ESI Mass Spectra of Cinchonas Formed from DHCD in the Enantioselective Hydrogenation of EtPy under Standard Conditions[a]

DHCD (mM/L)	Time (min)	Conversion (%)	*m/z* Values (relative peak intensity %) 297	299	301	307	ee (%)
0.001[a]	15	19	46	100	53	57	63
	40	40	36	63	64	100	51
0.01[a]	15	68	81	34	60	100	92
	30	97	36	56	56	100	91
0.1[b]	10	49	100	47	45	23	91
	20	99	10	20	50	100	92
1.0[b]	15	80	100	20	15	5	92
	25	100	100	55	30	10	92

[a] SIM—selective ion monitoring.
[b] SCAN.

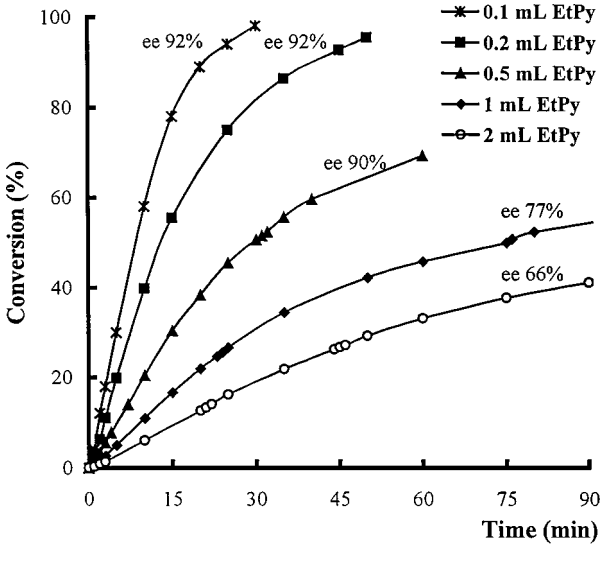

FIG. 5. Conversion and enantioselectivity as function of EtPy concentration on the hydrogenation of EtPy under standard conditions.

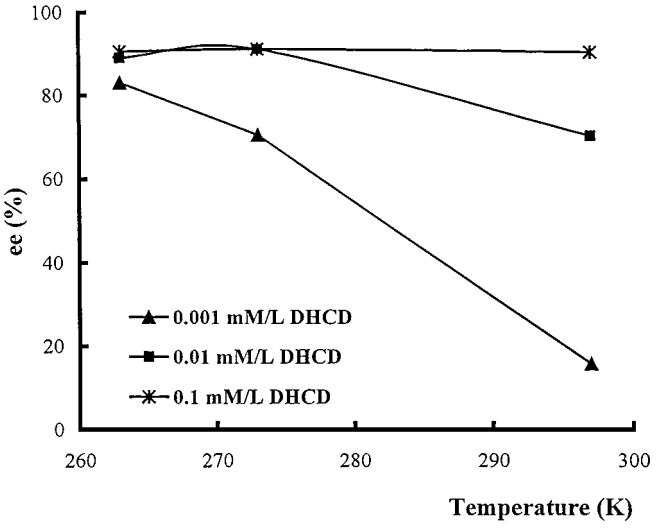

FIG. 6. Effect of the DHCD concentration and temperature for the hydrogenation of EtPy on optical yield (25 mg E 4759, 1 mL AcOH + 1 mL toluene in order to keep AcOH dissolved, 1 bar H_2, 0.5 mL EtPy).

The Effect of Alumina

Because of the discovery of the new type of aluminum compounds in AcOH, it was necessary to investigate the role of the alumina support on the hydrogenation of EtPy.

The experiments were carried out on support-free platinum (platinum black) as well as on a mechanical mixture of platinum and aluminum oxide, under standard conditions. The results are summarized in Figs. 8 and 9 and Table 5. It has to be noted that optimization was not among the aims of this study. For comparison, experimental data obtained on catalyst E 4759 on mixtures of $Pt + HOAl(OAc)_2$, $Pt + (HO)_2Al(OAc)$, and DHCD-free platinum (racemic hydrogenation) are also included.

TABLE 4

Reaction Time and Conversion as Functions of DHCD Concentration and Temperature[a]

	Reaction time (min)/conversion (%)		
DHCD (mM/L)	263 K	273 K	297 K
0.001	150/32	150/35	150/45
0.01	130/64	60/66	50/97
0.1	120/86	60/98	37/98

[a] For conditions see Fig. 6.

It is clearly seen that hydrogenation on Pt is significantly slower than that on a $Pt + Al_2O_3$ mixture and on mixtures of $Pt + HOAl(OAc)_2$ and $Pt + (HO)_2Al(OAc)$ containing an identical amount of Pt.

Our dry-box studies on the filtrate containing oxonium cations have so far yielded no appreciable results. It is possible that oxonium cations, being moisture sensitive, disappear during hydrogenation. In the presence of alumina, however, they are formed continuously.

Interpretation of the Enantioselective Hydrogenation of α-Ketoesters

Our new experimental data make it possible to complete the mechanism of chiral hydrogenation; for example, (i) the extremely low $DHCD/Pt_{surface}$ ratio for obtaining the

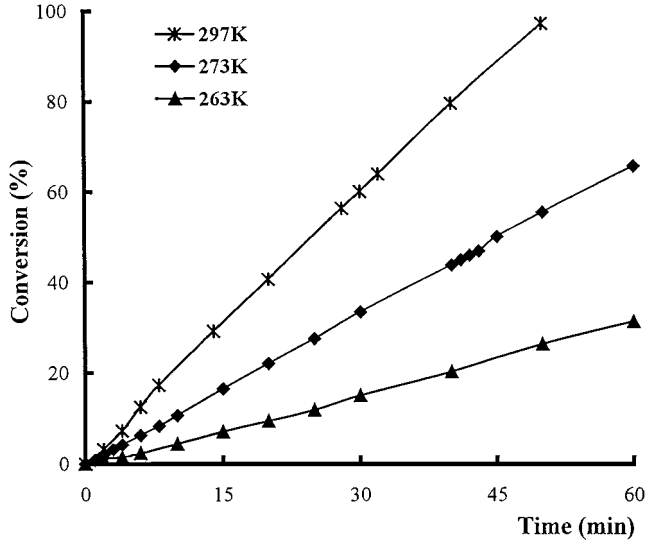

FIG. 7. Effect of the temperature for the hydrogenation of EtPy on the conversion (25 mg E 4759, 1 mL AcOH + 1 mL toluene, 1 bar H_2, 0.01 mM/L DHCD, 0.5 mL EtPy).

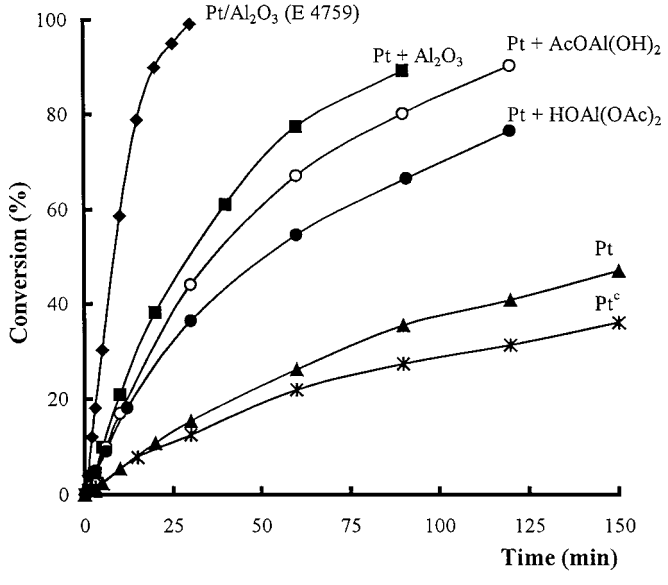

FIG. 8. Enantioselective hydrogenation of ethyl pyruvate on platinum black in acetic acid at room temperature (1.5 mg Pt, 0.01 mM/L dihydrocinchonidine). For abbreviations and conditions see Table 5.

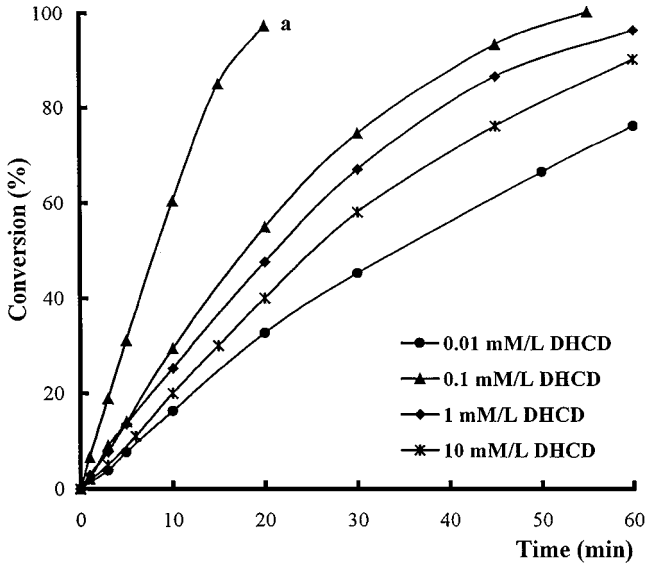

FIG. 9. Enantioselective hydrogenation of ethyl pyruvate over platinum black in acetic acid at room temperature (1.5 mg Pt, a, 5 mg Pt). For abbreviations and conditions see Table 5.

maximal ee; (ii) the new data obtained by platinum black + alumina mixture; (iii) in the course of the analysis of the products of the enantioselective hydrogenation of EtPy by ESI-MS, an unknown substance was detected in the mass spectrum at $m/z = 451$ with maximal abundance.

TABLE 5

Enantioselective Hydrogenation of Ethyl Pyruvate over Platinum in Acetic Acid at Room Temperature (2 ml of AcOH, hydrogen pressure: 1 bar, 0.1 mL ethyl pyruvate, stirring: 1200 rpm)

Catalyst[a]	Time	DHCD (mM/L)	Conversion (%)	ee (%)
1.5 mg Pt	150 min	0.01	40	45
	66 h[b]	0.01	84	38
	150 min[c]	0	36	0
1.5 mg Pt +	85 min	0.01	90	68
20 mg Al_2O_3	66 h[b]	0.01	99	64
	3 h[c]	0	60	0
1.5 mg Pt +	120 min	0.01	77	61
20 mg $HOAl(OAc)_2$				
1.5 mg Pt +	150 min	0.01	78	62
20 mg $AcOAl(OH)_2$				
1.5 mg Pt +	45 min	0.1	98	83
20 mg Al_2O_3	45 min	0.2	98	85
	60 min	0.4	98	81
	60 min	1	97	75
	60 min	10	60	67
5 mg Pt +	25 min	0.1	100	74
20 mg Al_2O_3	25 min	1	100	72
25 mg Pt/Al_2O_3(E 4759)	25 min	0.01	100	90

[a] Pt = Platinum black.
[b] Without stirring.
[c] Without dihydrocinchonidine.

According to earlier investigations the DHCD/$Pt_{surface}$ ratio = 0.1–1, depending on the solvent (5, 6). In AcOH at 303 K under 5.6 bar of hydrogen pressure this ratio was found to be 0.038 (12). According to Fig. 10 this value is 0.0072 (conditions: 25 mg E 4759, 2 mL AcOH, 1 bar hydrogen, 296 K, 0.1 mL EtPy, 0.006 mM/L DHCD, $Pt_{surface}$ = 0.00173 mM, DHCD = 0.0000125 mM). Accordingly, under our experimental conditions the minimal DHCD amount for obtaining the maximal ee is five times less than that determined in Ref. 12. We attempted to reproduce the experimental data reported by LeBlond *et al.* (12), using the 1% Pt–alumina catalyst purchased from Aldrich (i.e., the same as that used by LeBlond *et al.*); however, we did not succeed. One probable reason for our failure may be that the two 1% Pt–alumina catalysts come from different batches, and no information is available about their characteristics. On the other hand, experimental results from different laboratories using catalyst E 4759 are fully reproducible.

Suppose that adsorption of one DHCD molecule demands an area of 15 Pt atoms on the catalyst surface (5, 6). In the case of monolayer adsorption only 10% of the 0.00173 mM $Pt_{surface}$ will be covered by DHCD under our experimental conditions, while the ee obtained on this catalyst surpasses 90%. Thus on the remaining ~90% $Pt_{surface}$ which is not covered by DHCD the hydrogenation does not occur. This may be interpreted by the following explanation: the chiral active sites are formed on well-defined surface Pt atoms having a special coordination (corners, vertices, kinks) (4, 16, 54–56) by the adsorbed DHCD molecule, and the hydrogenation will proceed with a high reaction rate only on these centers. Accordingly, it

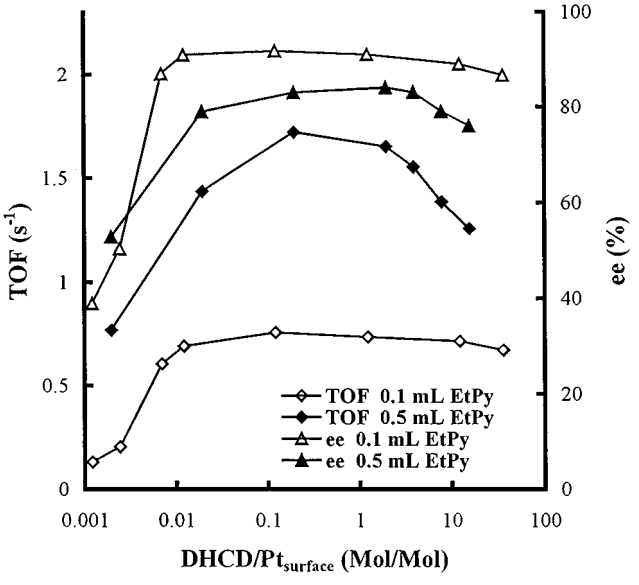

FIG. 10. Initial rate and enantioselectivity as functions of DHCD/$Pt_{surface}$ for hydrogenation of EtPy. For conditions and abbreviations, see Fig. 4.

seems that the sizes of the Pt clusters have no particular importance, as was concluded in previous studies (reviewed in Ref. 5). If the enantioselective hydrogenation were to proceed on edge and terrace atoms, then a significantly higher DHCD concentration would be necessary for obtaining high ee-s. In this context there are noteworthy studies by Augustine *et al.* (16) on the mechanism of the enantioselective hydrogenation. It is regrettable that in AcOH no such study has been carried out.

In the course of studies on the mechanisms of liquid-phase heterogeneous catalytic reactions, hydrogen deficiency at the catalytic sites must be taken into account (4). The dissociation of hydrogen on platinum proceeds at a significantly higher rate on edge sites and corner sites of the surface, which is where chiral active centers develop in the course of DHCD adsorption. Surface hydrogen rapidly reacts with polarized ethyl pyruvate at the site of generation, prior to migration to the terrace atoms. This means that even if adsorbed EtPy were available on the terrace atoms of platinum, no reaction would take place due to the hydrogen-deficient environment.

What is the role of the oxonium cation? Owing to its high reactivity, this electrophilic compound present both in the solution and on the surface of the catalyst may affect the chemical reaction. To the best of our knowledge, oxonium ions of this structure have not been described in the pertinent literature (see, e.g., the recently published monograph by Olah *et al.* (57)).

In acetic acid the oxonium cations may affect the chemical reaction in a hitherto unknown but most probably multiple fashion: oxonium cation removes impurities; it polarizes ethyl pyruvate; it stabilizes transition-state structures on platinum; it may have a role in the development of electrostatic potential on the surface. (It must also be kept in mind that the support itself (58) and/or the unknown substances present therein may also affect (increase or decrease) the reaction rate.)

In our opinion these cations make the so-called electrostatic catalysis (59) based on electrostatic acceleration (60) possible. The chiral sites and the electrostatic potential may be responsible for the increased rate of the chiral hydrogenation for the decrease of the activation energy, that is, for the catalysis. Molecular mechanics calculations, on the binding of the reacting molecules on crystal surfaces, should take place due to formation of a strong electrostatic field on the surface (59). If the polarity of the transition complex in a reaction is higher than that in the ground state, the electrostatic stabilization effect of the dipoles of the environment (in our case these are the cations) will increase the rate by electrostatic acceleration (60).

This possibility is confirmed by the presence of the molecular ion identifiable at $m/z = 747$ in the ESI–MS spectrum (Table 1), small amounts of which appear in the solution at high DHCD concentrations (above 1 mM/L). We think it is justified to assume that these species have a strong tendency to be adsorbed on the surface of both platinum and support.

CONCLUSION

By studying the optimization of the enantioselective hydrogenation of EtPy as a function of the DHCD concentration it could be established that on the catalyst under optimal conditions only 10% of the $Pt_{surface}$ is covered by DHCD. DHCD is adsorbed only at sites of higher coordination with a well-defined morphology (edges, corners), and hydrogenation may take place only at these locations. The rest of the Pt surface remains intact.

As regards the mechanism of the hydrogenation reaction, we emphasize the role of electrostatic acceleration rather than that of ligand acceleration, because the former allows the ionic character of the hydrogenation to be taken into account.

Furthermore, the present results suggest an explanation, entirely different from the currently accepted one, as to why acetic acid has proven to be the optimal solvent in the asymmetric hydrogenation of EtPy to EtLt, and why aluminum oxide is the optimal support for platinum.

Our future plan is the experimental verification of the presumed role of oxonium cations by the extensive investigation of their role in the hydrogenation of EtPy on mixed catalysts comprising platinum black and carefully characterized Al_2O_3 and SiO_2. A similarly important program is the isolation and preparation of the aluminum-containing oxonium cations.

ACKNOWLEDGMENTS

Financial support by the Hungarian National Science Foundation (OTKA Grant T031707) and the Hungarian Academy of Sciences (AKP 2000-20 2,4) is highly appreciated. We also thank Professor F. Notheisz for valuable discussions.

REFERENCES

1. Blaser, H.-U., and Müller, M., *Stud. Surf. Sci. Catal.* **59**, 73 (1991).
2. Jannes, G., and Dubois, V., Eds., "Chiral Reactions in Heterogeneous Catalysis." Plenum Press, New York, 1995.
3. Baiker, A., and Blaser, H.-U., *in*, "Handbook of Heterogeneous Catalysis" (G. Ertl, H. Knözinger, and J. Weitkamp, Eds.), Vol. 5. p. 2422. VCH, Weinheim, 1997.
4. Smith, G. V., and Notheisz, F., "Heterogeneous Catalysis in Organic Chemistry." Academic Press, New York, 1999.
5. Baiker, A., *J. Mol. Catal. A Chem.* **115**, 473 (1997).
6. Blaser, H.-U., Jalett, H.-P., Müller, M., and Studer, M., *Catal. Today* **37**, 441 (1997).
7. Török, B., Felföldi, K., Szakonyi, G., Balázsik, K., and Bartók, M., *Catal. Lett.* **52**, 81 (1998).
8. Zuo, X., Liu, H., Guo, D., and Yang, X., *Tetrahedron* **55**, 7787 (1999).
9. Bürgi, T., and Baiker, A., *J. Catal.* **194**, 445 (2000).
10. Bhaduri, S., Lahiri, G. K., Munshi, P., and Mukesh, D., *Catal. Lett.* **65**, 61 (2000).

11. Hall, T. J., Halder, J. E., Hutchings, G. J., Jenkins, R. L., Johnston, P., McMorn, P., Wells, P. B., and Wells, R. P. K., *Topics Catal.* **11/12**, 351 (2000).
12. LeBlond, C., Wang, J., Liu, J., Andrews, A. T., and Sun, Y.-K., *J. Am. Chem. Soc.* **121**, 4920 (1999); *Topics Catal.* **13**, 169 (2000).
13. Böhmer, U., Franke, F., Morgenschweis, K., Bieber, T., and Reschetilowski, W., *Catal. Today* **60**, 167 (2000).
14. Bartók, M., Szabó, P. T., Bartók, T., and Szöllösi, Gy., *Rapid Commun. Mass Spectrom.* **14**, 509 (2000).
15. Blaser, H.-U., Jalett, H.-P., Lottenbach, W., and Studer, M., *J. Am. Chem. Soc.* **122**, 12675 (2000).
16. Augustine, R. L., Tanielyan, S. K., and Doyle, L. K., *Tetrahedron Asymmetry* **4**, 1803 (1993).
17. Blaser, H.-U., Jalett, H.-P., Monti, D. M., Reber, J. F., and Wehrli, J. T., *Stud. Surf. Sci. Catal.* **41**, 153 (1988).
18. Wehrli, J. T., Baiker, A., Monti, D. M., and Blaser, H.-U., *J. Mol. Catal.* **61**, 207 (1990).
19. Blaser, H.-U., Jalett, H.-P., Monti, D. M., Baiker, A., and Wehrli, J. T., *Stud. Surf. Sci. Catal.* **67**, 147 (1991).
20. Jackson, S. D., Willis, J., McLellan, G. D., Webb, G., Keegan, M. B. T., Moyes, R. B., Simpson, S., Wells, P. B., and Whyman, R., *J. Catal.* **139**, 191 (1993).
21. Mallat, T., Frauchiger, S., Kooyman, P. J., Schürch, M., and Baiker, A., *Catal. Lett.* **63**, 121 (1999).
22. Collier, P. J., Iggo, J. A., and Whyman, R., *J. Mol. Catal. A Chem.* **146**, 149 (1999).
23. Simons, K. E., Meheux, P. A., Griffiths, S. P., Sutherland, I. M., Johnston, P., Wells, P. B., Carley, A. F., Rajumon, M. K., Roberts, M. W., and Ibbotson, A., *Recl. Trav. Chim. Pays-Bas* **113**, 465 (1994).
24. Carley, A. F., Rajumon, M. K., Roberts, M. W., and Wells, P. B., *J. Chem. Soc., Faraday Trans.* **91**, 2167 (1995).
25. Blaser, H.-U., Imhof, D., and Studer, M., *Stud. Surf. Sci. Catal.* **108**, 175 (1997).
26. Evans, T., Woodhead, A. P., Gutiérrez-Sosa, A., Thornton, G., Hall, T. J., Davis, A. A., Young, N. A., Wells, P. B., Oldman, R. J., Plashkevych, O., Vahtras, O., Ågren, H., and Carravetta, V., *Surf. Sci. Lett.* **436**, L691–L696 (1999).
27. Sutherland, I. M., Ibbotson, A., Moyes, R. B., and Wells, P. B., *J. Catal.* **125**, 77 (1990).
28. Bürgi, T., Atamny, F., Knop-Gericke, A., Hävecker, M., Schedel-Niedrig, T., Schlögl, R., and Baiker, A., *Catal. Lett.* **66**, 109 (2000).
29. Bürgi, T., Atamny, F., Schlögl, R., and Baiker, A., *J. Phys. Chem. B* **104**, 5953 (2000).
30. Bonello, J. M., Lambert, R. M., Künzle, N., and Baiker, A., *J. Am. Chem. Soc.* **122**, 9864 (2000).
31. Dijkstra, G. D. H., Kellogg, R. M., Wynberg, H., Svendsen, J. S., Marko, I., and Sharpless, K. B., *J. Am. Chem. Soc.* **111**, 8069 (1989).
32. Pfaltz, A., and Heinz, T., *Topics Catal.* **4**, 229 (1997).
33. Bürgi, T., and Baiker, A., *J. Am. Chem. Soc.* **120**, 12920 (1998).
34. Morawsky, V., Prüße, U., Witte, L., and. Vorlop, K.-D., *Catal. Commun.* **1**, 15 (2000).
35. Blaser, H.-U., Jalett, H.-P., Garland, M., Studer, M., Thies, H., and Wirth-Tijani, A., *J. Catal.* **173**, 282 (1998).
36. Tálas, E., Botz, L., Margitfalvi, J. L., Sticher, O., and Baiker, A., *J. Planar Chromatogr.* **5**, 28 (1992).
37. Margitfalvi, J. L., and Hegedüs, M., *J. Mol. Catal. A Chem.* **107**, 281 (1996).
38. Augustine, R. L., and Tanielyan, S. K., *J. Mol. Catal. A Chem.* **112**, 93 (1996).
39. Margitfalvi, J. L., Hegedüs, M., and Tfirst, E., *Tetrahedron Asymmetry* **7**, 571 (1996).
40. Bartók, M., Felföldi, K., Török, B., and Bartók, T., *Chem. Commun.* 2605 (1998).
41. Bartók, M., Felföldi, K., Szöllösi, Gy., and Bartók, T., *Catal. Lett.* **61**, 1 (1999).
42. Szöllösi, Gy., Felföldi, K., Bartók, T., and Bartók, M., *React. Kinet. Catal. Lett.* **71**, 99 (2000).
43. Blaser, H.-U., Garland, M., and Jalett, H.-P., *J. Catal.* **144**, 569 (1993).
44. Sun, Y., Landau, R. N., Wang, J., LeBlond, C., and Blackmond, D. G., *J. Am. Chem. Soc.* **118**, 1348 (1996).
45. Margitfalvi, J. L., Tálas, E., Tfirst, E., Kumar, C. V., and Gergely, A., *Appl. Catal. A Gen.* **191**, 177 (2000).
46. Fenn, J. B., Mann, M., Meng, C. K., Wong, S. F., and Whitehouse, C. M., *Science* **246**, 64 (1989).
47. Gaskell, S. J., *J. Mass Spectrom.* **32**, 677 (1997);
48. Kebarle, P., *J. Mass. Spectrom.* **32**, 922 (1997).
49. von Arx, M., Mallat, T., and Baiker, A., *J. Catal.* **193**, 161 (2000).
50. Kele, Z., Janáky, T., Mészáros, T., Fehér, A., Dudits, D., and Szabó, P. T., *Rapid Commun. Mass. Spectrom.* **12**, 1564 (1998).
51. Bartók, M., Szabó, P. T., Bartók, T., Szöllösi, Gy., and Balázsik, K., *Rapid Commun. Mass Spectrom.* **15**, 65 (2001).
52. Blaser, H.-U., and Garland, M., *J. Am. Chem. Soc.* **112**, 7048 (1990).
53. Meheux, P. A., Ibbotson, A., and Wells, P. B., *J. Catal.* **128**, 387 (1991).
54. Siegel, S., Outlaw, J., and Garti, N., *J. Catal.* **52**, 102 (1978).
55. Somorjai, G. A., "Chemistry Two Dimensions: Surfaces." Cornell Univ. Press, Ithaca, New York and London, 1981.
56. Augustine, R. L., and Warner, R. W., *J. Catal.* **80**, 358 (1983).
57. Olah, G. A., Laali, K. K., Wang Q., and Prakash, G. K. S., "Onium Ions." Wiley, New York, 1998.
58. Kropp, P. J., Daus, K. A., Tubergen, M. W., Kepler, K. D., Wilson, V. P., Craig, S. L., Baillargeon, M. M., and Breton, G. W., *J. Am. Chem. Soc.* **115**, 3071 (1993).
59. Náray-Szabó, G., *in* "Encyclopedia of Computational Chemistry" (P. v. R. Schleyer, Ed.), Vol. 1. Wiley, New York, 1998.
60. Jiao, H., and Schleyer, P. v. R., *J. Chem. Soc., Faraday Trans.* **90**, 1559 (1994).